Electron Cyclotron Emission from the Princeton Large Tokamak

J. Hosea, V. Arunasalam, and R. Cano[a]
Plasma Physics Laboratory, Princeton University, Princeton, New Jersey 08540
(Received 8 July 1977)

Experimental measurements of electron cyclotron emission from the Princeton Large Tokamak plasma reveal that blackbody emission occurs at the fundamental frequency. Such emission, not possible by direct thermal excitation of electromagnetic waves, is herein attributed to thermal excitation of electrostatic (Bernstein) waves which then mode convert into electromagnetic waves. The local feature of the electrostatic wave generation permits spatially and temporally resolved measurements of electron temperature as for the second-harmonic emission.

In fusion research there is considerable interest in understanding the emission near the electron cyclotron frequency f_{ce} and its harmonics. Such emission could constitute a significant power loss in a reactor,[1] can prescribe the proper conditions for efficient application of electron cyclotron resonance (ECR) heating through the reverse process (Kirchhoff's radiation law[2]), and, of more immediate interest, can provide an independent measurement of the properties of the emitting electrons[2,3] (e.g., electron temperature T_e and/or presence of runaways). In tokamak regimes for which the runaway population is small, the emission near the second and higher harmonics can be well understood[4] in terms of either the conventional hot-plasma theory[5] or the single-particle emission theory.[2] However, emission near the fundamental frequency[4] ($f \approx f_{ce}$) is found to be much larger than predicted by the hot-plasma theory for direct electromagnetic-wave emission. Such emission should be negligible compared to the balckbody value of κT_e per mode[6] since in the vicinity of the cyclotron frequency the electromagnetic wave is almost circularly polarized with its sense of rotation opposite to that of the gyrating electrons.

In this Letter, we first present experimental evidence which demonstrates that in Princeton Large Tokamak (PLT) discharges with a sufficiently low runaway population, the emission near f_{ce}, when viewed from the inside of the torus, is indeed blackbody emission from the cyclotron layer [$f \approx f_{ce}(R)$ where R is the major radius of the emitting layer]. We then show that this emission can be attributed to thermal excitation of electrostatic Bernstein waves which undergo mode conversion into electromagnetic waves, rather than to direct thermal excitation of electromagnetic waves. Hence, detection of blackbody emission at f_{ce}, as well as as $2f_{ce}$,[7,8] gives a local time-resolved measurement of $T_e(R, t)$ as will be illustrated.

In this study, we compare the detected emission at $f \approx f_{ce}$ with that at $f \approx 2f_{ce}$ which has previously been shown to be blackbody under the conditions set by the conventional hot-plasma theory.[7,8] Receiving antennas (horn or a horn-lens combination as to be noted) are located in the equatorial plane along the major radius and are oriented to receive extraordinary waves. Conventional superheterodyne detectors are used since these permit the optimum spatial resolution along R of the various detection schemes. For these systems, the output signals are proportional to the emitted power. That is, $P = \kappa T_e(R) \Delta f (1 - e^{-\tau})$, where τ is the optical depth of the emitting layer[2] ($\tau \gtrsim 2$ for black-body emission), and Δf is the receiver bandwidth.

In Fig. 1(a), we present f_{ce} and $2f_{ce}$ emission profiles versus position along the major radius for the discharge conditions noted. ($R = R_0 + r$ where $R_0 = 132$ cm is the nominal major radius at the center of the plasma.) These data were obtained by setting the receiver frequencies at 70 GHz (f_{ce}) and 140 GHz ($2f_{ce}$) and placing the emitting layer at the desired R or r by choosing the appropriate magnetic field level $B_\phi(R_0)$. The spatial resolution for each receiver is set by its bandwidth $\Delta f \approx 400$ MHz which gives layer thicknesses of $\Delta R \approx 0.8$ cm (f_{ce}) and 0.4 cm ($2f_{ce}$), and by the lobe widths $\Delta\theta \approx \pm 6.5°$ (f_{ce}) and $\pm 4°$ ($2f_{ce}$) of simple horn antennas located at $r = -50$ cm [spot diameters are $d \approx 11$ cm (f_{ce}) and 7 cm ($2f_{ce}$) at R_0]. For comparison, the average temperature profile obtained from Thomson scattering along a vertical line through the plasma is also shown in Fig. 1(a).

As found previously,[7,8] the $2f_{ce}$ emission profile is in good agreement with the Thomson-scattering profile as expected for blackbody emission (the

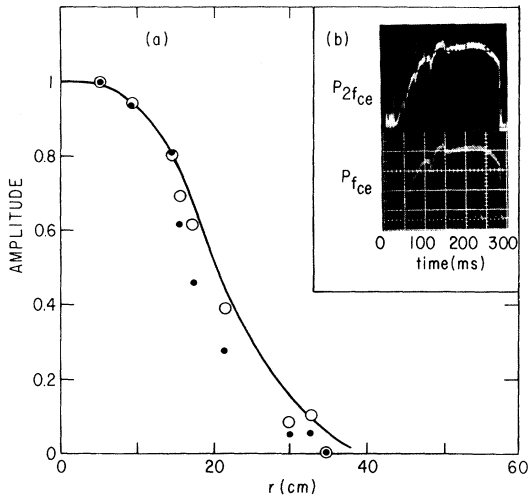

FIG. 1. (a) Cyclotron emission profiles at $t = 100$ msec for f_{ce} (●) and $2f_{ce}$ (○) emission. The average Thomson-scattering profile (—) is shown for comparison [$T_e(0) \approx 1$ keV, $n_e = 3\times10^{13}$ cm^{-3} $(1-r^2/40^2)$]. (b) Emission vs time at $r = 5$ cm.

hot-plasma theory[9] gives $\tau \sim 10$ at $r = 5$ cm decreasing to $\tau \sim 1$ at $r = 30$ cm). The $2f_{ce}$ profile falls somewhat below the Thomson-scattering profile at larger r partly because of an observed overall reduction in T_e as B_φ was decreased, and partly because the detection spot size weights the emission toward larger r (i.e., lower T_e).

Clearly, the f_{ce} emission profile is in good accord with the $2f_{ce}$ emission profile. Again, the difference between these profiles at larger r can be attributed to the different spot sizes of the detectors. Furthermore, the time evolution of the emission at f_{ce} is identical to that at $2f_{ce}$ as illustrated in Fig. 1(b); and, indeed, within the experimental accuracy of our receiver calibrations $P_{2f_{ce}}/P_{f_{ce}} \approx 1$ as expected for the approximately one-dimensional character of our antennas. This one-to-one space-time correspondence between the f_{ce} and $2f_{ce}$ emission demonstrates that the f_{ce} emission is both blackbody and generated at the $f = f_{ce}(R)$ layer.

This result is in sharp contrast to the spectral measurements of Costley and co-workers,[4,10] for which the ratio $P_{2f_{ce}}/P_{f_{ce}}$ varied between ~ 2 and ~ 8, instead of remaining at a fixed value of $\sim 2(2f_{ce}/f_{ce})^2 = 8$. We believe that this discrepancy between our results and theirs is due first to the fact that our antennas are approximately one-dimensional and select only the extraordinary polarization, and secondly, to the fact that we detect the f_{ce} emission from the accessible side of the plasma.

The balckbody emission near f_{ce} can be explained with the following theoretical model. By thermal excitation, electrostatic Bernstein waves build up to their blackbody value of κT_e per mode near the cyclotron layer in accordance with the equipartition theorem.[2] These waves propagate towards the upper hybrid layer (lower B_φ) and undergo complete mode conversion into extraordinary electromagnetic waves near the upper hybrid layer. Finally, the electromagnetic waves then propagate in the direction of increasing B_φ, cross the cyclotron layer with negligible attenuation, and reach the antenna at the inside of the torus. In the literature, it has been shown analytically[6,11] and by numerical solution of the wave equations[12] that when the Bernstein wave is completely absorbed in the vicinity of the cyclotron layer, an extraordinary electromagnetic wave with $f \sim f_{ce}$, incident on the plasma from the accessible side, undergoes complete mode conversion into the Bernstein wave. Hence, the reverse process (our model) is clearly viable provided that the region near the cyclotron layer is optically thick (i.e., black) for Bernstein waves.

From the electrostatic dispersion relation for a collisionless hot plasma {Eqs. (7.13)–(7.17) and (7.21) of Bekefi[2] [see also Eq. (9.103) of Stix[5]]} and taking account of the effects of the relativistic mass increase,[13] one can show that for large $\alpha_n = (2\pi/k_\parallel v_T)(f + nf_{ce})$ and $\lambda = k_\perp^2 v_T^2/8\pi^2 f_{ce}^2$, the real ($k_{\perp R}$) and imaginary ($k_{\perp I}$) components of the Bernstein-wave propagation constant with $f \approx f_{ce}$ may be written

$$k_{\perp R} \approx \left(\frac{4}{\pi^{1/2}}\right)^{1/3} \frac{2\pi f_{ce}}{v_T} \left[\frac{f_{pe}^2}{f^2 - (f_{ce} - \Delta f_{ce})^2}\right]^{1/3}, \quad (1)$$

$$k_{\perp I} \approx (16\pi^{9/2} f_{pe}^2 f_{ce}^2 / k_{\perp R}^2 v_T^3) A. \quad (2)$$

Here $\perp$ and $\parallel$ refer to directions perpendicular and parallel, respectively, to the magnetic field, $v_T^2 = 2\kappa T_e/m$, $\Delta f_{ce} \approx f_{ce} v_T^2/c^2$ is the average relativistic decrease in the cyclotron frequency, and the line-shape function A is given by[14]

$$A \approx \frac{2\pi^{1/2}}{k_\parallel v_T} \exp\left[\frac{-4\pi^2 (f - f_{ce})^2}{k_\parallel^2 v_T^2}\right] \quad (3)$$

for $k_\parallel v_T > 2\pi \Delta f_{ce}$, or

$$A \approx \frac{4c^3 f}{\pi^{1/2} v_T^3 f_{ce}^2} \left(\frac{1 - f^2}{f_{ce}^2}\right)^{1/2} \exp\left[-\left(\frac{1 - f^2}{f_{ce}^2}\right)\frac{c^2}{v_T^2}\right], \quad (4)$$

for $k_\parallel v_T < 2\pi \Delta f_{ce}$. The value of $k_\parallel$ below which damping due to relativistic broadening [Eq. (4)] outweighs that due to the usual cyclotron damping

[Eq. (3)] is $k_{\parallel}/k_0 \approx v_T/c$ (e.g., ~0.06 for $T_e = 1$ keV) where $k_0 = 2\pi f_{ce}/c$.

It may be noted from Eq. (4) that the relativistic line broadening is highly asymmetric and occurs only for $f \lesssim f_{ce}$. It is apparent from Eqs. (1)–(4) that the heavily damped Bernstein waves propagating along R have their frequencies in the range $f_{ce} - \Delta f_{ce} \approx f_{ce}(1 - v_T^2/c^2) \lesssim f \lesssim f_{ce}$.

The optical depth for Bernstein waves in a tokamak plasma ($B \propto 1/R$) is then

$$\tau = \int_0^l 2k_{\perp I}\, dl \approx a\pi^{1/2}(2\pi)^{7/3} \frac{Rf_{ce}}{c}\left(\frac{f_{pe}^2 v_T}{f_{ce}^2 c}\right)^{1/3}, \qquad (5)$$

where $a \approx 1$ in the small $k_{\parallel}$ case of Eq. (3), and $a \approx (8/\pi\epsilon)^{1/2}$ for the relativistic line-broadening case of Eq. (4). Here ϵ is the Naperian base. This optical depth is a weak function of density and temperature, and for the data of Fig. 1, Eq. (5) gives $5 \times 10^3 \lesssim \tau \lesssim 10^4$. Thus, the condition for blackbody Bernstein-wave emission near the cyclotron layer is well satisfied and leads us to conclude that indeed the model we have described governs the fundamental emission.

The localization of the Bernstein wave generation permits local temperature measurement at $f_{ce}(R)$ with a spatial resolution (ΔR) similar to that obtained at $2f_{ce}(R)$. Blackbody conditions are less restrictive at f_{ce} and the reduction in the receiver frequency facilitates frequency sweeping to obtain $T_e(r)$ repetitively during a single discharge. However, for accessibility the detecting antenna of f_{ce} emission must be placed at the inside of the torus whereas inside and outside locations are equivalent for the $2f_{ce}$ emission.

Cyclotron-emission detection at both f_{ce} and $2f_{ce}$ is a powerful method not only for measuring the temperature profile, but also for making time-resolved studies of local perturbations in the electron temperature due to instabilities and/or electron heating. In Fig. 2, we present examples of temperature fluctuations due to magnetohydrodynamic (MHD) activity in PLT measured at f_{ce} and $2f_{ce}$. The $m = 0$ sawtooth relaxations presumably precipitated by $m = 1$ MHD oscillations inside the rational magnetic surface[15] $q(r) = rB_\varphi/R_0B_\theta(r) = 1$ are shown in Fig. 2(a) (with an amplitude consistent with soft x-ray measurements[8]), and $m = 2$ oscillations in the vicinity of the $q = 2$ layer are shown in Fig. 2(b). For the $2f_{ce}$ data of Fig. 2(b), a horn-lens antenna at the outside of the plasma was used ($r = +50$ cm), and hence the f_{ce} and $2f_{ce}$ oscillations are in phase as expected for $m = 2$, since the horns are $\varphi = 180°$

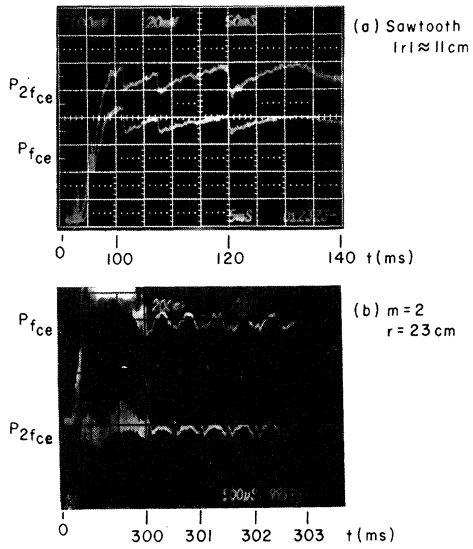

FIG. 2. Local MHD temperature fluctuations in PLT discharges.

apart around the torus (toroidal mode number $n = 1$). The structure imposed by the $m = 2$ magnetic island on the temperature oscillations at the given minor circumference is clearly evident on the $2f_{ce}$ emission (viewed over an ~3-cm spot size) and is discernible on the f_{ce} emission (the f_{ce} spot size of ~16.5 cm here can be considerably reduced with the addition of a lens). The amplitudes and wave forms of the $m = 2$ oscillations of the f_{ce} and $2f_{ce}$ emissions tracked very closely throughout a discharge and with changes in magnetic field, even though they were very sensitive to the selected position relative to the $q = 2$ layer. Thus, this comparison affords additional proof that the f_{ce} emission is blackbody emission and comes from the cyclotron layer as opposed to the upper hybrid layer.

In conclusion we wish to emphasize that our results show that the f_{ce} emission is blackbody emission and the emission measurements at f_{ce} and $2f_{ce}$ indeed provide a powerful diagnostic tool in tokamak fusion research. We have demonstrated that by this method one can measure not only the temperature profiles but also the local MHD temperature fluctuations. We believe that our experimental and theoretical demonstration of the blackbody nature of the cyclotron layer lends significant support to the use of ECR auxiliary heating in tokamaks.

The authors would like to acknowledge the valuable assistance received from the members of the PLT group. Special thanks are due the Thom-

son Scattering group which provided temperature profiles for comparison. This work was supported by the U. S. Energy Research and Development Administration, Contract No. EY-76-C-02-3073.

[a]Permanent address: Centre d'Etudes Nucléaires, Fontenay-aux-Roses, France.

[1]M. N. Rosenbluth, Nucl. Fusion 10, 340 (1970).-
[2]G. Bekefi, *Radiation Proceeses in a Plasma* (Wiley, New York, 1966).
[3]F. Engelmann and M. Curatoto, Nucl. Fusion 13, 497 (1973).
[4]A. E. Costley, R. J. Hastie, J. W. M. Paul, and J. Chamberlain, Phys. Rev. Lett. 33, 758 (1974); TFR Group and NPL Submillimeter Wave Group, in *Proceedings of the Seventh European Conference on Controlled Fusion and Plasma Physics, Lausanne, Switzerland, 1975* (European Physical Society, Geneva, 1975), Paper 14a.
[5]T. H. Stix, *The Theory of Plasma Waves* (McGraw-Hill, New York, 1962).
[6]I. Fidone and G. Granata, Phys. Fluids 10, 1885 (1973).
[7]TFR Group, in *Proceedings of the Seventh European Conference on Controlled Fusion and Plasma Physics, Lausanne, Switzerland, 1975* (European Physical Society, Geneva, 1975), Paper 14b.
[8]J. Hosea and V. Arunasalam, Bull. Am. Phys. Soc. 21, 1159 (1976).
[9]V. Arunasalam, E. B. Meservey, M. N. Gurnee, and R. C. Davidson, Phys. Fluids 11, 1076 (1968).
[10]A. E. Costley and TFR Group, Phys. Rev. Lett. 38, 1477 (1977).
[11]T. H. Stix, Phys. Rev. Lett. 15, 878 (1975).
[12]J. J. Schuss and J. C. Hosea, Phys. Fluids 18, 727 (1975).
[13]Yu. N. Dnestrovskii, D. P. Kostomarov, and N. V. Skrydlov, Zh. Tekh. Fiz. 33, 922 (1963) [Sov. Phys. Tech. Phys. 8, 691 (1964)].
[14]There are no transit-time broadening effects for collective normal modes of systems (such as Bernstein modes) or for thermodynamic blackbody emission.
[15]S. von Goeler, W. Stodiek, and N. Sauthoff, Phys. Rev. Lett. 33, 1201 (1974).

Island-Dissolution Phase Transition in a Chemisorbed Layer

T.-M. Lu, G.-C. Wang, and M. G. Lagally
Materials Science Center, University of Wisconsin, Madison, Wisconsin 53706
(Received 22 March 1977)

A phase transition has been observed in O chemisorbed on W(110) at low coverages, with a transition temperature ~ 250°K lower than that observed for saturation coverage W(110)$p(2\times1)$-O. This transition is interpreted in terms of two-dimensional dissolution of islands. A fit to lattice-gas models for both low and saturation coverage allows separate determination of the attractive and repulsive adatom-adatom interactions, and gives values of -0.069 and 0.15 eV/atom, respectively.

The study of phase changes in overlayers is an important tool in understanding the interactions that adatoms undergo.[1] Very little work has been done on chemisorption systems, and only H/W(100)[2] and O/W(110)[3] have been studied in any detail. This Letter reports a new phase transition for O/W(110) at low coverages. We observe what we believe to be two-dimensional dissolution of the chemisorbed islands previously identified in this system.[3,4] As a result, we are able to determine separately attractive and repulsive adatom-adatom interaction energies leading to the $p(2\times1)$ structure.

The experiment[3] consists of measuring the superlattice beam intensities and angular profiles in low-energy electron diffraction (LEED) from the W(110) surface covered with varying amounts of oxygen. The most important feature of this system is that the ordered overlayer forms by an island-growth mechanism. This is established by the observation that superlattice LEED beams form already at very low coverage.[4] It implies a net attractive adatom-adatom interaction. However, the $p(2\times1)$ structure that is formed, shown in Fig. 1 and consisting of doubly spaced close-packed rows parallel to ⟨111⟩ directions, requires a nearest-neighbor repulsion. Streaking of spots is not observed in the diffraction pattern during formation of the overlayer.[3,4a,5] This implies that island formation is preferred over the formation of long rows, and therefore that the attractive interactions along ⟨111⟩ directions are about equal in magnitude[5,6] and considerably smaller than the nearest-neighbor repulsion that prevents close packing.

Oxygen-coverage determinations were made by

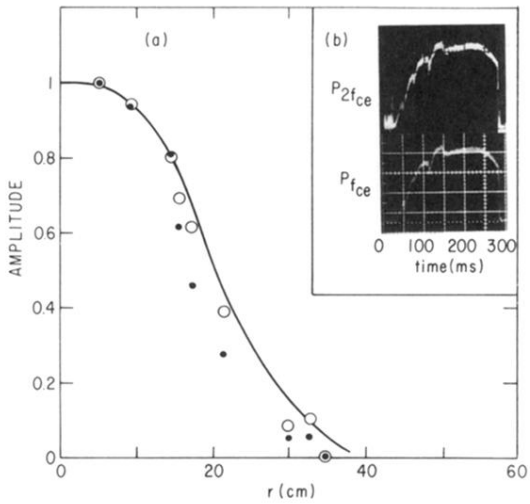

FIG. 1. (a) Cyclotron emission profiles at $t = 100$ msec for f_{ce} (●) and $2f_{ce}$ (○) emission. The average Thomson-scattering profile (—) is shown for comparison [$T_e(0) \approx 1$ keV, $n_e = 3\times 10^{13}$ cm^{-3} $(1 - r^2/40^2)$]. (b) Emission vs time at $r = 5$ cm.

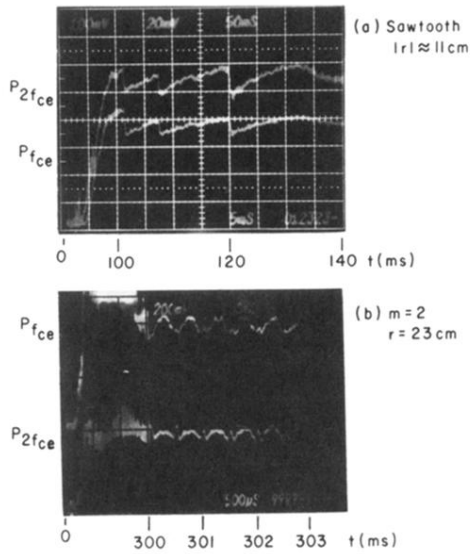

FIG. 2. Local MHD temperature fluctuations in PLT discharges.